T2R2 東京科学大学 リサーチリポジトリ
Science Tokyo Research Repository

論文 / 著書情報
Article / Book Information

Title(English)	Changes in electrical resistivity track changes in tectonic plate coupling
Authors(English)	Heise, W., T. G. Caldwell, E.A. Bertrand, G.J. Hill, S.L. Bennie, Y. Ogawa
Citation(English)	Geophysical Research Letters, Vol. 40, , p. 1-5
Pub. date	2013, 10

Powered by T2R2 (Science Tokyo Research Repository)

GEOPHYSICAL RESEARCH LETTERS, VOL. 40, 1–5, doi:10.1002/grl.50959, 2013

Changes in electrical resistivity track changes in tectonic plate coupling

Wiebke Heise,[1] T. Grant Caldwell,[1] Edward A. Bertrand,[1] Graham J. Hill,[1]
Stewart L. Bennie,[1] and Yasuo Ogawa[2]

Received 14 August 2013; accepted 12 September 2013.

[1] Interplate coupling on the Hikurangi subduction margin along the east coast of New Zealand's North Island changes north to south from almost uncoupled to locked. Clay-rich sediments and aqueous fluids at the subduction interface have been invoked as key factors in the frictional processes that control interplate coupling. Here we use magnetotelluric data to show that the subduction interface in the weakly coupled region is electrically conductive but is resistive in the locked region. These results indicate the presence of a layer of fluid- and clay-rich sediments in the weakly coupled region and support the idea that the presence of fluid and hydrated clays at the interface is a major factor controlling plate coupling. **Citation:** Heise, W., T. G. Caldwell, E. A. Bertrand, G. J. Hill, S. L. Bennie, and Y. Ogawa (2013), Changes in electrical resistivity track changes in tectonic plate coupling, *Geophys. Res. Lett.*, *40*, doi:10.1002/grl.50959.

1. Introduction

[2] The *M*9 2011 Tohoku-Oki earthquake demonstrated that current understanding of the frictional properties of the subduction interface is incomplete. During this earthquake, parts of the subduction interface that had previously undergone slow slip [e.g., *Ito et al*., 2013; *Kato et al*., 2012] and were expected to act as barriers to rupture propagation also ruptured [*Noda and Lapusta*, 2013]. On the Hikurangi subduction margin along the east coast of New Zealand's North Island, GPS data show that interplate coupling changes along the margin from very weakly coupled in the north to strongly coupled (or locked) in the south. Several studies [e.g., *Schwartz and Rokosky*, 2007; *Wallace and Beavan*, 2010, *Faulkner et al*., 2011] suggest that clay-rich sediments and aqueous fluids play a key role in plate coupling. The presence of clay-rich sediments at the subduction interface has recently been offered as a possible explanation for the dynamic weakening of parts of the Tohoku-Oki subduction interface that failed in 2011 and that had been assumed to be creeping [*Noda and Lapusta*, 2013].

[3] Changes in interplate coupling are thought to result from a combination of the effects of plate structure, the presence or absence of sediment at the interface, temperature, stress regime, and fluid pressure [e.g., *McCaffrey et al*., 2008, *Wallace et al*., 2009]. In particular, the 350°C isotherm has often been taken to mark the downdip transition from strong to weak interplate coupling [*Hyndman and Wang*, 1993; *McCaffrey et al*., 2008]. However, in the northern part of the Hikurangi margin, the plate interface is weakly coupled at depths that are too shallow and too cold to be caused by temperature [*McCaffrey et al*., 2008]. Also, the abrupt change in the interplate coupling observed along the Hikurangi margin (Figure 1) is not easily explained by changes in thermal structure alone [*McCaffrey et al*., 2008].

[4] Other mechanisms controlling friction at the plate interface invoke the presence of overpressured fluid; fluids have been proposed as a key causative factor in the occurrence of slow slip events (SSEs) [*Schwartz and Rokosky*, 2007; *Liu and Rice*, 2007]. Twenty-four SSEs have been observed along the Hikurangi margin since continuous GPS recording commenced in 2000, all but one of which are located in the region where the coupling is weak [*Wallace et al*., 2012]. Seismological evidence for the presence of overpressured fluids on a subduction interface has also been reported at several subduction margins where SSEs occur [e.g., *Ito et al*., 2007; *Kodaira et al*., 2004], including the northern part of the Hikurangi margin [*Reyners et al*., 1999]. Seismic tremor, thought to represent slip on the plate interface that is too small to be resolved in GPS data, has been described as representing "fluid-enabled shear slip" [*Shelly et al*., 2006] and has been linked to areas of high fluid content in seismic reflection data at the Cascadia subduction margin [*Kao et al*., 2006, *Calvert et al*., 2011]. Finally, magnetotelluric (MT) data from the northern part of the Hikurangi margin [*Heise et al*., 2012] show that the plate interface just north and downdip of a large SSE in 2010 (Figure 2) is electrically conductive. *Heise et al*. [2012] interpret the high conductivity as a zone of underplated sediments and a region of upward fluid transport along the plate interface.

[5] In general, the MT data are much more sensitive to the presence or absence of small amounts of interconnected fluid than seismological methods. Here we report new MT data from the locked part of the Hikurangi margin and from the weakly coupled area where tremor was located [*Kim et al*., 2011] during the 2010 SSE (Figure 2). *Umeda et al*. [2006] also noted that low-frequency tremor beneath the Kii Peninsula in SW Japan is associated with a lower crustal conductive zone above the subduction interface.

2. Magnetotelluric Data and Analysis

[6] The MT method uses surface recordings of fluctuations in the Earth's electromagnetic field over a wide period range to infer the electrical resistivity of the subsurface down to depths of ~50 km for the period range (0.01 to 680 s) of the data discussed here. The amplitude and phase relations between the surface electromagnetic field components that

Additional supporting information may be found in the online version of this article.

[1]GNS Science, Lower Hutt, New Zealand.
[2]Volcanic Fluid Research Center, Tokyo Institute of Technology, Tokyo, Japan.

Corresponding author: W. Heise, GNS Science, Lower Hutt, New Zealand. (w.heise@gns.cri.nz)

©2013. American Geophysical Union. All Rights Reserved.
0094-8276/13/10.1002/grl.50959

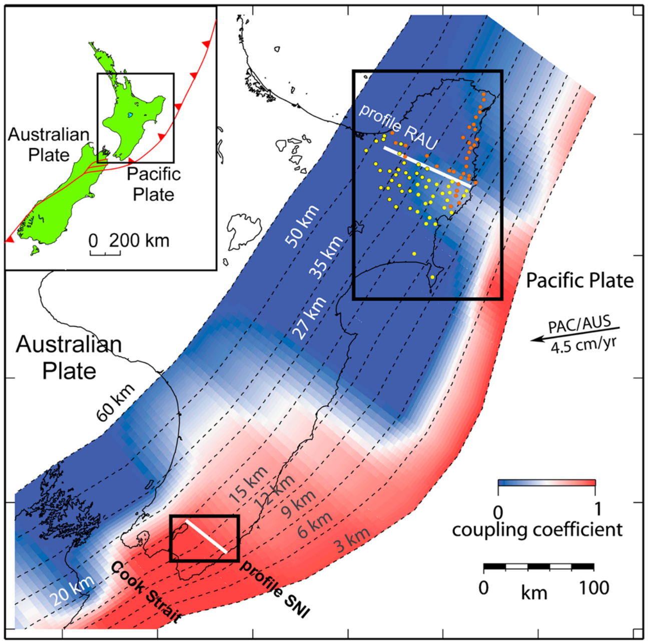

Figure 1. Map of Hikurangi subduction interface plate coupling with a coupling coefficient of 1 being fully locked [*Wallace and Beavan*, 2010]. Dashed contours show the depth to the subduction interface. The black arrow shows the motion of the Australian Plate relative to the Pacific Plate in the North Island. The black boxes mark the two study areas. Locations of the MT measurements in the northern part of the Hikurangi margin are shown by orange and yellow dots measured in 2009 and 2011–2012, respectively. White lines show the locations of the model cross sections shown in Figure 4.

form the MT data are expressed in the frequency domain by the "impedance tensor" **Z** and the "induction vector" **K. Z** and K are complex transfer functions that relate the horizontal electric (**E**) field vector and the vertical component of the magnetic field (H_z) to the horizontal magnetic field components (**H**), respectively. The transfer functions are defined by the equations $\mathbf{E} = \mathbf{ZH}$ and $H_z = -\mathbf{K}$H and represent the normalized response of the Earth to a vertically incident plane wave magnetic field excitation.

[7] While the magnitude relations in the impedance tensor data can be strongly distorted by localized conductivity heterogeneities near the surface, the phase relationships are unaffected and provide a direct indication of the lateral and vertical resistivity changes in a depth range that depends on the period and overlying resistivity. This phase relationship depends on polarization and is a tensor $\mathbf{\Phi} = \mathbf{X}^{-1}\mathbf{Y}$, where **X** and **Y** are respectively the real and imaginary parts of **Z** [*Caldwell et al.*, 2004]. This 2-D tensor can be represented graphically by an ellipse; the ellipse axes show the orientation and the relative magnitude of the tensor principal values Φ_{max} and Φ_{min}. Differences in the magnitude and the orientation of the tensor principal values thus provide a way of directly visualizing resistivity gradients present at depth.

[8] In Figures 2 and 3, we use the geometric mean $\Phi_2 = \sqrt{(\Phi_{max}\Phi_{min})}$ of the principal values to indicate the magnitude of the phase tensor response. In simple (quasi 1-D) situations, decreasing resistivity with increasing depth is indicated by values of $\Phi_2 > 45°$. Where a phase tensor analysis of the data identifies a 1-D section at short periods, the case for almost the entire data set discussed here, the phase mixing effects of any near-surface distortion on the impedance can be removed from the impedance data prior to inversion [*Bibby et al.*, 2005].

3. Results

[9] Maps of phase tensor ellipses at 28 s period for both the southern and northern MT surveys are shown in Figures 2 and 3. In the northern, uncoupled part of the margin, 50 new MT soundings were added to the MT survey reported in *Heise et al.* [2012]. High (>45°) Φ_2 values (warm colors) near the east coast indicate the presence of a thick layer of conductive sediments, while the high phases in the west (where resistive basement rocks are exposed at the surface) suggest the presence of a conductor at depth.

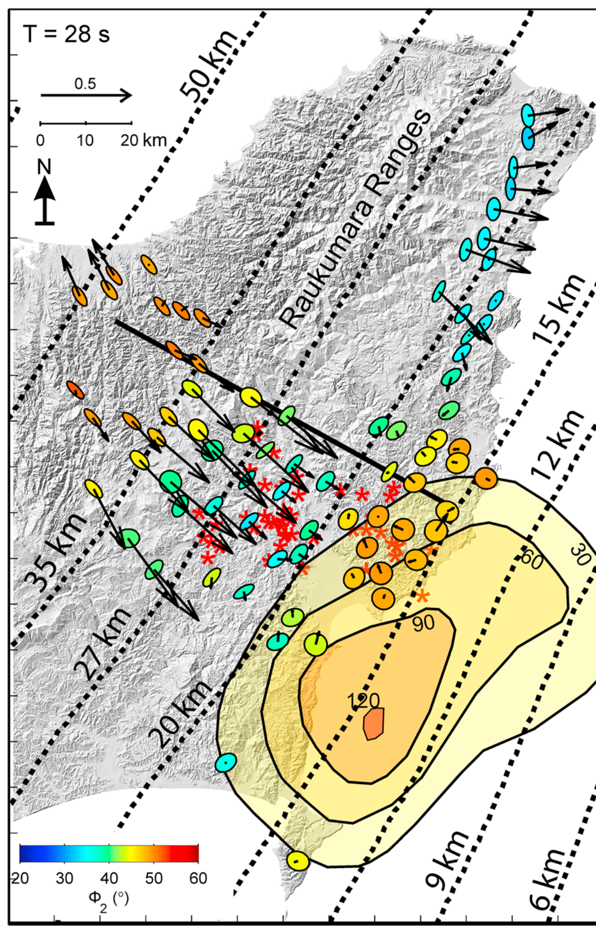

Figure 2. Map of phase tensor ellipses and induction vectors for the northern Hikurangi margin. The phase tensor ellipse sizes have been normalized by their major axis (Φ_{max}). The color fill shows Φ_2. Dashed lines show the depth to the subduction interface. Black contours show the total slip (in mm), and red stars show the locations of seismic tremor associated with the 2010 SSE [*Kim et al.*, 2011]. The black line shows the location of the model cross section shown in Figure 4b.

[10] In the locked part of the margin in the south, 24 broadband MT soundings were recorded on a single profile approximately perpendicular to the strike of the subducting plate and where the plate interface is between 10 and 20 km deep (Figure 3). The along-profile change in the phase tensor orientation (Figure 3) indicates a strong 3-D response (Figure S1 in the supporting information) reflecting the influence of the seawater in Cook Strait (Figure 1). Higher Φ_2 values near the coast suggest that conductive rocks are present close to the coast.

4. 3-D Inverse Modeling

[11] The relationship between the MT data and the resistivity is inherently nonlinear, and inversion methods must be used to create a model of the resistivity structure. Although the data from the southern part of the margin are restricted to a single profile, the 3-D nature of the observed response requires a 3-D approach to data inversion. We used the 3-D inversion algorithm of *Siripunvaraporn et al.* [2005] to invert the data from both regions (for details, see the supporting information).

[12] The resistivity model for the southern line of measurements is shown in Figure 4a. Three near-surface conductive areas (~3 Ωm) mark small basins of quaternary sediment [*Begg and Johnston*, 2000], the low resistivity reflecting the high clay and fluid content of the sediments. Only at its southeastern end are resistivities less than 50 Ωm observed at deeper levels (C1 and C2 in Figure 4a). These conductors (C1 and C2) are interpreted to show fluids released from dewatering sediments associated with the accretionary prism present offshore. A similar feature was observed in the MT data from a profile across the northern part of the South Island [*Wannamaker et al*., 2009.]. Note, in particular, that the crust above the plate interface northwest of C1 and C2 is resistive (~300 Ωm).

[13] In the weakly coupled part of the Hikurangi margin in the north, analysis of earlier MT data [*Heise et al*., 2012] showed that a conductive zone is present above the plate interface. In Figure 4b, we show a slice through an updated 3-D resistivity model of the same region incorporating additional data from 50 MT soundings. The new measurements encompass the area in which seismic tremor has been

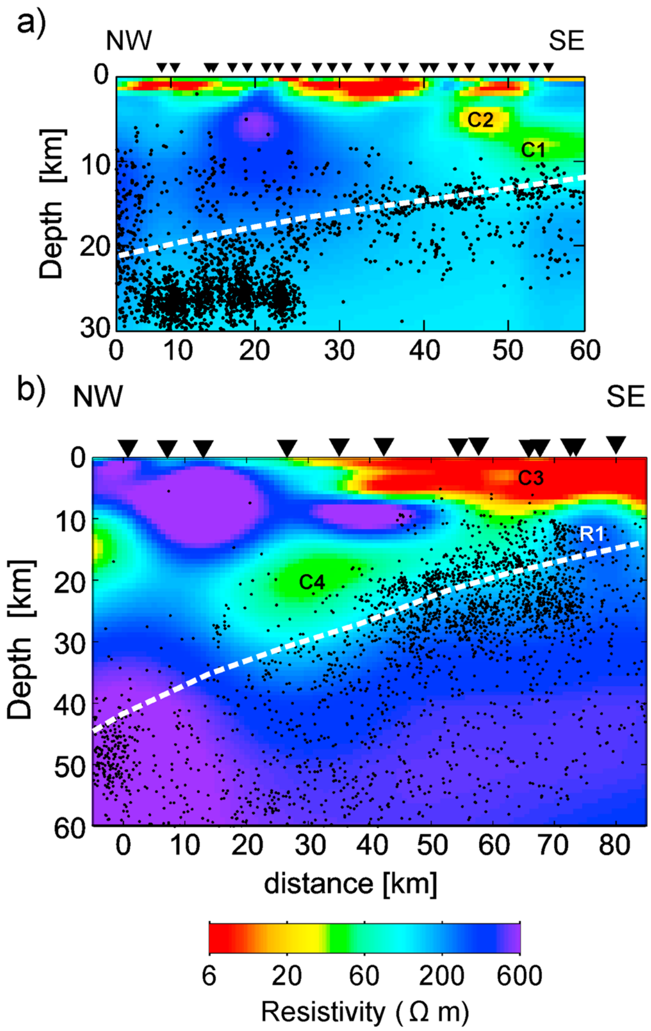

Figure 4. (a) Slice through the 3-D resistivity model along the profile in the southern part of the Hikurangi margin (Figure 2). Black dots show relocated earthquake hypocenters within 25 km of this profile [*Reyners et al*., 2011]. The dashed white line shows the plate interface [*Reyners and Eberhart-Phillips*, 2009]. (b) Slice through the 3-D resistivity model from the northern part of the Hikurangi margin (Figure 2). The dashed white line shows the plate interface [*Reyners et al*., 2011].

located [*Kim et al*., 2011] (Figure 2). This model shows two conductive features: a layer of highly conductive material marking the thick (~8 km) sequence of marine sediments present near the east coast and a less conductive zone above the plate interface confirming the results of our earlier study [*Heise et al*., 2012]. The new data also show that the zone above the subducting plate is conductive in the area where seismic tremor was located (Figure 2) during the 2010 SSE [*Kim et al*., 2011]. Note that the resistive zone above the plate interface updip of the area of tremor (R1 in Figure 4b) is a localized feature that is not present on nearby parallel slices through the 3-D model volume.

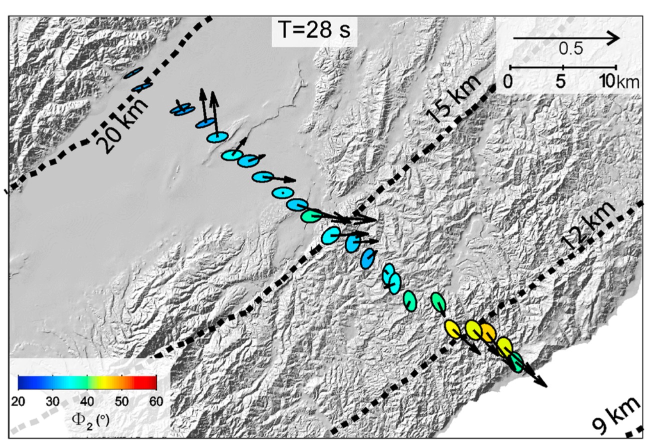

Figure 3. Phase tensor ellipses and induction vectors at the southern part of the Hikurangi margin. Other features as in Figure 2.

5. Discussion

[14] The difference in the resistivity structure above the subduction interface between the weakly and strongly coupled

parts of the Hikurangi margin is remarkable. While the MT data will not resolve a thin conductive zone (e.g., a thin clay-rich layer of fault gouge), hypothesis testing (Figures S5 and S6 in the supporting information) shows that a dipping conductor similar in conductance (i.e., the conductivity thickness product) to that present above the plate interface in the northern part of the margin would be resolved by our data on the southern line if present. Thus, the MT data are consistent with a layer of conductive underplated sediments above the plate interface in the north (C4 in Figure 4b) but not in the south. *Heise et al*. [2012] interpreted the dipping conductive layer above the interface in the north to mark a zone of fluid-rich underplated sediment.

[15] This inference is in good accord with the structure of the margin. In the north, where the convergence rate is 50–60 mm/yr [*Wallace et al*., 2004], the margin is erosional while in the south, where the convergence rate is smaller (20–30 mm/yr), sediment is accumulating offshore in an accretionary prism [*Barnes and Mercier de Lepinay*, 1997].

[16] There is other geologic and seismological evidence for the subduction and underplating of sediment in the northern part of the Hikurangi margin [*Walcott*, 1987; *Reyners et al*., 1999; *Eberhart-Phillips and Reyners*, 1999; *Bassett et al*., 2010]. In particular, *Reyners et al*. [1999] showed that anomalously high *P* wave to *S* wave velocity ratios occur above the subduction interface within a zone of crustal *P* wave velocities, consistent with the presence of overpressured fluid within a layer of subducted sediment.

[17] In Figure 4b, the resistivities in the southeast within the upper ~8 km (C3) are ~3 Ωm reflecting the high fluid and clay (in particular smectite) content of the marine sediments [*Darby*, 2002; *Mazengarb and Speden*, 2000]. Below ~8 km, resistivity values increase to >30 Ωm in the dipping conductive layer (C4) above the interface. *Heise et al*. [2012] argued that the increase in resistivity, which seems to occur with the onset of seismicity, reflects the transformation of smectite to illite [*Vrolijk*, 1990; *Hyndman et al*., 1995] and/or the increase in cementation [*Moore et al*., 2007] within the downgoing sediments. Thus, both illitic clays and saline fluids may be the cause of the conductance within the dipping layer. However, since MT data best resolve the conductance, the layer resistivity and thickness are not separately determinable, and we cannot rule out the possibility that interconnected fluids alone, perhaps overpressured and hosted in connected fractures, might explain the increased conductivity.

6. Conclusions

[18] The difference in plate coupling and resistivity structure between the northern and southern parts of the Hikurangi margin suggest that the presence of a conductive layer of fluid- and/or clay-rich sediments may play an important, perhaps dominant, role in controlling the frictional processes at the interface and thus the interseismic coupling.

[19] Although large subduction earthquakes may not be able to nucleate within a weakly coupled patch of the subduction interface [*Faulkner et al*., 2011; *Noda and Lapusta*, 2013], the presence of a layer of fluid- and clay-rich sediments on the interface may make the propagation of an earthquake rupture into and through such parts of the interface more favorable due to coseismic weakening. If this inference is correct, the likelihood of a margin-spanning earthquake on the Hikurangi margin is greater than currently recognized [*Stirling et al*., 2012]. Confirmation that sediments and/or overpressured fluid control the frictional properties of the subduction interface has important ramifications for subduction margin hazard because the tacit assumption has generally been that weakly coupled parts of the interface are unlikely to dynamically rupture in a large earthquake.

[20] **Acknowledgments.** We would like to thank Weerachi Siripunvarporn for making his 3-D inverse modeling code available for this research. Susan Ellis, Martin Reyners, and Phaedra Upton provided comments on an earlier version of this paper. Insightful reviews by Yoshihiro Ito and Harold Tobin also helped us clarify the ideas presented here. This work was funded from GNS Science's direct Crown funding and a Marsden research grant from the Royal Society of New Zealand.

[21] The Editor thanks Harold Tobin and Yoshihiro Ito for their assistance in evaluating this paper.

References

Barnes, P. M., and B. Mercier de Lepinay (1997), Rates and mechanics of rapid frontal accretion along the very obliquely convergent southern Hikurangi margin, New Zealand, *J. Geophys. Res.*, *102*, 24,931–24,952.

Bassett, D., R. Sutherland, S. Henrys, T. Stern, M. Scherwath, A. Benson, S. Toulmin, and M. Henderson (2010), Three-dimensional velocity structure of the northern Hikurangi margin, Raukumara, New Zealand: Implications for the growth of continental crust by subduction erosion and tectonic underplating, *Geochem. Geophys. Geosyst.*, *11*, Q10013, doi:10.1029/2010GC003137.

Begg, J. G., and M. R. Johnston (compilers) (2000), Geology of the Wellington area. Institute of Geological & Nuclear Sciences 1:250 000 geological map 10. 1 sheet + 64p. Lower Hutt, *New Zealand. Institute of Geological & Nuclear Sciences Limited*.

Bibby, H. M., T. G. Caldwell, and C. Brown (2005), Determinable and non-determinable parameters of galvanic distortion in magnetotellurics, *Geophys. J. Int.*, *163*, 915–930.

Caldwell, T. G., H. M. Bibby, and C. Brown (2004), The magnetotelluric phase tensor, *Geophys. J. Int.*, *158*, 457–469.

Calvert, A. J., L. A. Preston, and A. M. Farahbod (2011), Sedimentary underplating at the Cascadia mantle-wedge corner revealed by seismic imaging, *Nat. Geosci.*, *4*, 545–548.

Darby, D. (2002), Seal properties, overpressure and stress in the Taranaki and East Coast Basins, New Zealand. *New Zealand Petroleum Conference* (*2002*: *Auckland*, *NZ*). 2002. pp. 363-372.

Eberhart-Philips, D., and M. Reyners (1999), Plate interface properties in the northeast Hikurangi subduction zone, New Zealand, from converted seismic waves, *Geophys. Res. Lett.*, *26*, 2565–2568.

Faulkner, D. R., T. M. Mitchell, J. Behnsen, T. Hirose, and T. Shimamoto (2011), Stuck in the mud? Earthquake nucleation and propagation through accretionary forearcs, *Geophys. Res. Lett.*, *38*, L18303, doi:10.1029/2011GL048552.

Heise, W., T. G. Caldwell, G. J. Hill, S. L. Bennie, and E. A. Bertrand (2012), Magnetotelluric imaging of fluid processes at the subduction interface of the Hikurangi margin, New Zealand, *Geophys. Res. Lett.*, *39*, L04308, doi:10.1029/2011GL050150.

Hyndman, R. D., and K. Wang (1993), Thermal constraints on the zone of major thrust earthquake failure: The Cascadia subduction zone, *J. Geophys. Res.*, *98*, 2039–2060.

Hyndman, R. D., K. Wang, and M. Yamano (1995), Thermal constraints on the seismogenic portion of the southwestern Japan subduction thrust, *J. Geophys. Res.*, *100*, 15,373–15,392.

Ito, Y., K. Obara, K. Shiomi, S. Sekine, and H. Hirose (2007), Slow earthquakes coincident with episodic tremors and slow slip events, *Science*, *26*, 503–506.

Ito, Y., et al. (2013), Episodic slow slip events in the Japan subduction zone before the 2011 Tohoku-Oki earthquake, *Tectonophysics*, *600*, 14–26.

Kao, H., S. Shan, H. Dragert, G. Rogers, J. F. Cassidy, K. Wang, T. James, and K. Ramachandran (2006), Spatial-temporal patterns of seismic tremors in northern Cascadia, *J. Geophys. Res.*, *111*, B03309, doi:10.1029/2005JB003727.

Kato, A., K. Obara, T. Igarashi, H. Tsuruoka, S. Nakagawa, and N. Hirata (2012), Propagation of slow slip leading up to the 2011Mw 9.0 Tohoku-Oki earthquake, *Science*, *335*, 705–708, doi:10.1126/science.1215141.

Kim, M. Y., S. Y. Schwartz, and S. Bannister (2011), Non-volcanic tremor associated with the March 2010 Gisborne slow slip event at the Hikurangi subduction margin, New Zealand. *Geophys. Res. Lett.*, *38*, L14301, doi:10.1029/2011GL048400.

Kodaira, S., T. Iidaka, A. Kato, J.-O. Park, T. Iwasaki, and Y. Kaneda (2004), High pore fluid pressure may cause silent slip in the Nankai Trough, *Science*, *304*, 1295–1299.

Liu, Y., and J. R. Rice (2007), Spontaneous and triggered aseismic deformation transients in a subduction fault model, *J. Geophys. Res.*, *112*, B09404, doi:10.1029/2007JB004930.

Mazengarb, C., and I. G. Speden (compilers) (2000), Geology of the Raukumara area: scale 1:250,000. Lower Hutt: Institute of Geological & Nuclear Sciences Limited. Institute of Geological & Nuclear Sciences 1:250,000 geological map.

McCaffrey, R., L. M. Wallace, and J. Beavan (2008), Slow slip and frictional transition at low temperature at the Hikurangi subduction zone, *Nat. Geosci.*, *1*, 316–320.

Moore, J. C., C. D. Rowe, and F. Meneghini (2007), How accretionary prisms elucidate seismogenesis in subduction zones, in *The Seismogenic Zone of Subduction Thrust Faults*, edited by T. H. Dixon and J. C. Moore, pp. 288–315, Columbia Univ. Press, New York.

Noda, H., and N. Lapusta (2013), Stable creeping fault segments can become destructive as a result of dynamic weakening, *Nature*, doi:10.1038/nature11703.

Reyners, M. E., and D. Eberhart-Phillips (2009), Small earthquakes provide insight into plate coupling and fluid distribution in the Hikurangi subduction zone, New Zealand, *Earth Planet. Sci. Lett.*, *282*, 299–305, doi:10.1016/j.epsl.2009.03.034.

Reyners, M. E., D. Eberhart-Phillips, and G. Stuart (1999), A three-dimensional image of shallow subduction: crustal structure of the Raukumara Peninsula, New Zealand, *Geophys. J. Int.*, *13*, 873–890.

Reyners, M., D. Eberhart-Phillips, and S. Bannister (2011), Tracking repeated subduction of the Hikurangi Plateau beneath New Zealand, *Earth Planet. Sci. Lett.*, *311*, 165–171, doi:10.1016/j.epsl.2011.09.011.

Schwartz, S. Y., and J. M. Rokosky (2007), Slow slip events and seismic tremor at circum-pacific subduction zones, *Rev. Geophys.*, *45*, RG3004, doi:10.1029/2006RG000208.

Shelly, D. R., G. C. Beroza, S. Ide, and S. Nakamula (2006), Low frequency earthquakes in Shikoku, Japan, and their relationship to episodic tremor and slip, *Nature*, *442*, 188–191, doi:10.1038/nature04931.

Siripunvaraporn, W., G. Egbert, Y. Lenbury, and M. Uyeshima (2005), Three-Dimensional Magnetotelluric: Data Space Method, *Phys. Earth Planet. Inter.*, *150*, 3–14.

Stirling, M. W., et al. (2012), National seismic hazard model for New Zealand: 2010 update, *Bull. Seism. Soc. Am.*, *102*, 1514–1542, doi:10.1785/0120110170.

Umeda, K., Y. Ogawa, K. Asamori, and T. Oikawa (2006), Aqueous fluids derived from a subducting slab: Observed high He emanation and conductive anomaly in a non-volcanic region, Kii Peninsula southwest Japan, *J. Volcanol. Geotherm. Res.*, *149*, 47–61.

Vrolijk, P. (1990), On the mechanical role of smectite in subduction zones, *Geology*, *18*, 703–707.

Walcott, R. I. (1987), Geodetic strain and the deformational history of the North Island during the late Cainozoic, *Phil. Trans. R. Soc. Lond.*, *A321*, 163–181.

Wallace, L. M., and R. J. Beavan (2010), Diverse slow slip behavior at the Hikurangi subduction margin, New Zealand. *J. Geophys. Res.*, *115*, B12402, doi:10.1029/2010JB007717.

Wallace, L., J. Beavan, R. McCaffrey, and D. Darby (2004), Subduction zone coupling and tectonic block rotations in the North Island, New Zealand. *J. Geophys. Res.*, *109*, B12406, doi:10.1029/2004JB003241.

Wallace, L. M., et al. (2009), Characterizing the seismogenic zone of a major plate boundary subduction thrust: Hikurangi Margin, New Zealand. *Geochem. Geophys. Geosyst. 10*, Q10006, doi:10.1029/2009GC002610.

Wallace, L. M., R. J. Beavan, S. C. Bannister, and C. A. Williams (2012), Simultaneous long-term and short-term slow slip events at the Hikurangi subduction margin, New Zealand: implications for processes that control slow slip event occurrence, duration, and migration. *J. Geophys. Res.*, *117*, B11402, doi:10.1029/2012JB009489.

Wannamaker, P. E., T. G. Caldwell, G. R. Jiracek, V. Maris, G. J. Hill, Y. Ogawa, H. M. Bibby, S. L. Bennie, and W. Heise (2009), Fluid and deformation regime of an advancing subduction system at Marlborough, New Zealand, *Nature*, doi:10.1038/nature08204.